

UCSF

UC San Francisco Electronic Theses and Dissertations

Title

Metabolic Pathway Changes Associated with the Development of Castrate Resistant Prostate Cancer

Permalink

<https://escholarship.org/uc/item/6dt1j48b>

Author

Chang, Kevin Chihow

Publication Date

2017

Peer reviewed|Thesis/dissertation

Metabolic Pathway Changes Associated with the Development of
Castrate Resistant Prostate Cancer

by

Kevin Chang

THESIS

Submitted in partial satisfaction of the requirements for the degree of

MASTER OF SCIENCE

in


Biomedical Imaging

in the

GRADUATE DIVISION

of the

UNIVERSITY OF CALIFORNIA, SAN FRANCISCO

Approved: 

Acknowledgements

Thanks to Dr. John Kurhanewicz, Dr. Renuka Sriram, and Jinny Sun for helping develop this project and guiding me through the day to day of the research

Thanks to my thesis committee – Dr. Kurhanewicz, Dr. Sriram, Dr. Bok, and Dr. Aggarwal – for their invaluable feedback and support regarding the project

Thanks to the rest of the Kurhanewicz Lab for making me feel welcome on a daily basis

Thanks to the MSBI program directors and administrators that made this thesis project possible

Metabolic Pathway Changes Associated with the Development of Castrate Resistant Prostate Cancer

Kevin Chang

Abstract: Metabolic reprogramming is known to occur with development and progression of prostate cancer. Based on preliminary studies, it is hypothesized that changes in metabolism will also predict, at an early time, whether men with prostate cancer are developing resistance to a common form of therapy, androgen deprivation therapy. Early knowledge of resistance would allow more effective intervention with secondary therapies. Hyperpolarized MRI (hpMRI) is a promising new metabolic MRI technique that allows the *in vivo* real-time assessment of metabolism in patients. In order to identify hpMRI metabolic probes for assessing resistance to ADT, this study used a NMR based metabolic approach to investigate changes in metabolic pathways with the development of resistance in the TRAMP murine model of prostate cancer. Infusion of uniformly labeled ^{13}C glucose allowed for the NMR analysis of metabolites (lactate, glutamate, alanine) in three key pathways (glycolysis, TCA cycle and amino acid synthesis). To accomplish this, two methods of metabolite extraction, the methanol/chloroform/water extraction and the perchloric acid extraction, were explored. High resolution 1D proton NMR, carbon-decoupled NMR, TOCSY, and HSQC analysis allowed for calculation of fractional enrichment, comparing androgen sensitive with resistant tumors. Overall, the perchloric acid extraction method was more time-consuming and less reproducible, so the methanol/chloroform/water extraction was chosen to be optimized further. Fractional enrichment calculations revealed that lactate fractional enrichment increased from 34.59% to 41.30%, glutamate increased from 8.16% to 9.27%, and alanine increased from undetectable to 37.13%. The increase in every biomarker, especially the dramatic increase in alanine, suggests that these may be appropriate targets for future

hyperpolarized studies using [1- C^{13}]pyruvate and [2- C^{13}]pyruvate to track lactate, alanine, and glutamate.

Table of Contents

1. Introduction	1
a. Clinical Motivation	1
b. Background	1
c. ¹³ C labeled Metabolic Substrate Studies.....	2
d. NMR Spectroscopy	3
2. Materials and Methods	7
a. TRAMP Murine Model.....	7
b. Uniformly-Labeled ¹³ C Glucose Infusion.....	7
c. Metabolite Extraction.....	8
d. NMR Experiments	9
e. NMR Analysis	9
3. Results	11
4. Discussion.....	16
5. Conclusion.....	17
6. References	18

List of Tables

Table 1: Measured Concentrations in the Spectra With and Without ^{13}C Decoupling.	13
Table 2: Fractional Enrichments for Lactate, Glutamate, And Alanine.	14

List of Figures

Figure 1: Metabolic Pathway Diagram.....	3
Figure 2: TOCSY Satellite Peak Patterns Based on Location of ^{13}C label [10].....	5
Figure 3: Alkyl region of the Stacked Extraction 1D Proton NMR spectra.....	11
Figure 4: Alkyl region of Stacked Decoupling 1D Proton NMR spectra.....	12
Figure 5: TOCSY Data Centered On Region Of Interest.....	13
Figure 6: Relevant Regions of HSQC Spectra.....	15
Figure 7: Comparisons of Relative Concentration Ratios from HSQC.....	15

1. Introduction

a. Clinical Motivation

Prostate cancer is the most commonly diagnosed cancer in men in the United States, with an estimated 161,360 new cases and 27,150 deaths in 2017 [1]. The main treatments for patients with advanced prostate cancer or suspected metastases are various androgen deprivation therapies (ADT) [2]. Though most patients initially respond well to androgen deprivation therapy, initiated at the time suspected metastases, eventually the cancer resumes growth. This emergence of therapeutic resistance and the continual growth despite castrate-level serum testosterone signals the onset of metastatic Castrate Resistant Prostate Cancer (CRPC), which is currently incurable [3], [4]. Prediction and identification of this transition from androgen sensitive cancer to CRPC will allow for improved treatment planning and prevent patients from bearing the side effects and financial burden of continuing ineffective ADT treatments, as well as support ongoing drug and imaging discovery efforts.

b. Background

Metabolomics refers to the study of the metabolites of an organism. The alteration of metabolism in cancer has long been known, since Otto Warburg discovered his eponymous effect [5]. Studying and comparing the relative activity of metabolic pathways can provide insight into these alterations, which correspond to changes made in regulation at the gene or protein level. One promising metabolic imaging technology is hyperpolarized MRI (hpMRI), which allows for over 10,000 fold increase in ^{13}C signal [6] and the imaging of *in vivo* metabolism in patients [7]. Application of hpMRI metabolic imaging using hyperpolarized ^{13}C -labeled metabolic probes requires the identification of metabolic biomarkers which can serve as readouts of specific pathways important

cancer evolution, progression and response to therapy. This can be accomplished through NMR based metabolomics NMR studies of ^{13}C labeled metabolic substrate studies.

c. ^{13}C labeled Metabolic Substrate Studies

Introduction of a high concentration of stable ^{13}C -labeled metabolic substrate, such as uniformly ^{13}C labeled glucose, to cells, tissues or an *in vivo* murine model allows for NMR detection of the metabolic products of these ^{13}C -labeled substrates, and therefore metabolic fluxes through key pathways. The ^{13}C -label of the substrates are incorporated through enzymatic conversion associated with different metabolic pathways into metabolic products; these metabolic substrates and their products can be extracted from the tissue using various metabolite extraction methods. One well described method is the methanol/chloroform/water extraction. Methanol and water are used to extract hydrophilic metabolites, and chloroform extracts hydrophobic metabolites, while proteins precipitate in between the two layers. However, there exists literature which suggests that for certain metabolites like glutamate, perchloric acid extractions may have higher extraction efficiency and reduce macromolecular interference from the baseline [8], [9]. Thus, this study will investigate and compare both methods.

A useful ^{13}C labeled metabolic substrate is uniformly labeled glucose, because of its ubiquitous consumption in the body, and participation in various anabolic and catabolic pathways. The three pathways specifically investigated in this study are amino acid synthesis using ^{13}C labeled alanine as a readout, aerobic glycolysis using ^{13}C labeled lactate as a readout, and the tricarboxylic acid (TCA) cycle using ^{13}C labeled glutamate as a readout, as depicted in Fig 1. Moreover, these three metabolites are ideal targets since they are downstream products of pyruvate, and can thus be detected by hyperpolarized $[1-^{13}\text{C}]$ pyruvate and $[2-^{13}\text{C}]$ pyruvate, the first of which is already approved for clinical use.

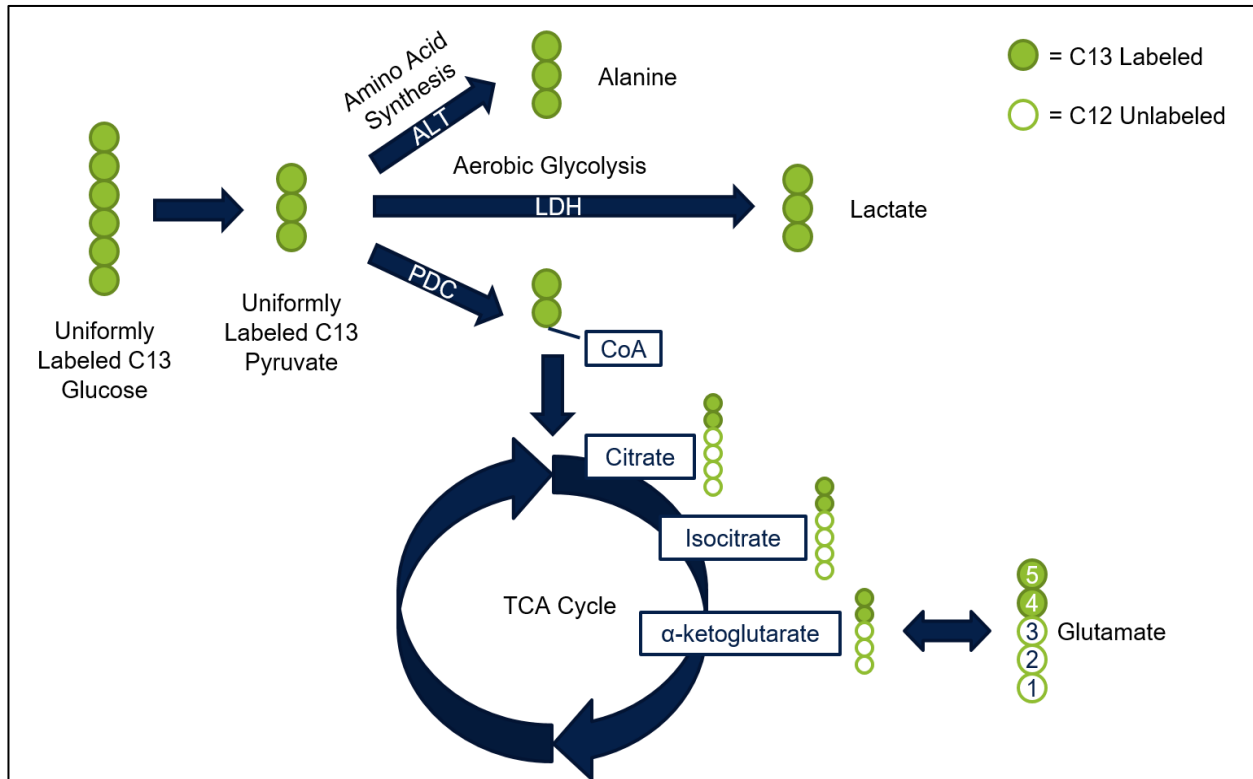


Figure 1: Metabolic pathway diagram representing the movement of ^{13}C labels across the amino acid synthesis, aerobic glycolysis, and TCA cycle pathways. The number labels in glutamate indicate which carbon positions will be labeled after one turn of the TCA cycle.

d. NMR Spectroscopy

NMR spectroscopy, or nuclear magnetic resonance spectroscopy, is a technique which takes advantage of the inherent spin of isotopes with an odd number of nucleons, such as ^1H or ^{13}C . When placed in a magnetic field of strength B_0 , NMR sensitive nuclei can absorb electromagnetic radiation at the characteristic frequency of the isotope, ν_0 . B_0 and ν_0 are related by the following equation

$$\nu_0 = \gamma B_0$$

where γ is a constant referred to as the gyromagnetic ratio of the particle. This magnetization can be excited by an RF pulse, which allows for detection of signal over time. The Fourier Transform

converts this into signal across different frequencies. Different nuclei will produce signal peaks at different frequencies based on their chemical shift, which results from the slightly different electronic environments each nuclei experiences.

In addition, peaks in the NMR spectra may experience splitting into multiple peaks centered at the chemical shift. This splitting is caused by interactions of spins of nuclei linked in a spin system, or J-coupling. By careful analysis of the peak signal intensities and frequencies and comparison with the known spectra of compounds of interest, NMR spectroscopy can provide a method for analyzing relative concentrations of said compounds.

The splitting that results from the coupling between the detected proton signal and the ^{13}C will be the main method of analyzing pathway flux in this study. Because the natural abundance of ^{13}C is so low (1.1%), nearly all of the signal from peaks split by ^{13}C will arise from the ^{13}C label chemically placed in the labeled metabolic substrate and in the subsequent labeled metabolic products. For example, the lactate methyl group signal of $[1-^{13}\text{C}]\text{lactate}$ should manifest as three distinct doublet peaks. The center doublet represents the unlabeled lactate; it does not demonstrate any splitting due to adjacent ^{13}C coupling and appears as a doublet due to the proton on the adjacent carbon. The two satellite peaks represent the splitting caused by the presence of ^{13}C label in the C3 methyl position of lactate, and flank the center peak with a distance of J_{CH} between them, where J_{CH} is the characteristic coupling constant between the lactate methyl protons and the labeled carbon. For the C3 lactate position, the J_{CH} is 127.5 ppm. The ability to visualize the unlabeled and ^{13}C labeled lactate pools in the 1D proton spectra allows for the calculation of fractional enrichment, or the percent of the total concentration that is ^{13}C labeled. Fractional enrichment, which can be calculated as

$$F = \frac{A(\text{satellites})}{A(\text{satellites}) + A(\text{central peak})}$$

where A is the integrated peak area, provides a simple method for comparing the relative activity of metabolic pathways [10].

However, it may be difficult to resolve peaks unambiguously when overlap between peaks of different metabolites occurs in 1D proton spectra.

One method to improve resolution is to increase the dimensionality of the study, from a 1D spectra to a 2D. 2D NMR takes advantage of coupling to produce cross peaks between two linked nuclei. Total Correlation Spectroscopy (TOCSY) produces proton-proton cross peaks based on interactions within a spin system. TOCSY is useful in that it produces characteristic patterns of satellite peaks spread out in two dimensions based on the labeling

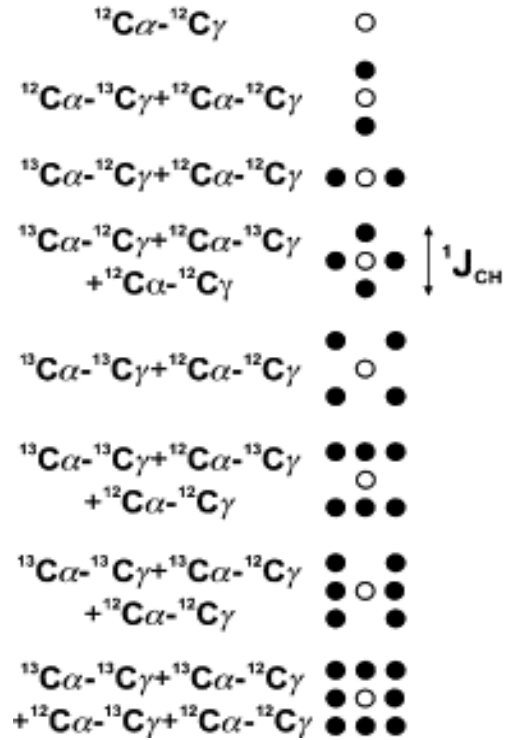


Figure 2: TOCSY satellite peak patterns based on location of ^{13}C label [11]

pattern, as seen in Fig 2, from Lane et al [11]. Fractional enrichment can be calculated using a similar equation as in the 1D spectra,

$$F = \frac{V(\text{satellites})}{V(\text{satellites}) + V(\text{central peak})}$$

only with integrated peak volumes instead of areas [10]. Heteronuclear Single Quantum Correlation (HSQC), in contrast, detects correlations between protons and the adjacent ^{13}C labeled

carbon. This provides a method for detecting only the ^{13}C labeled species and examining the relative concentrations between them.

Together, these different NMR techniques were applied in this study to the metabolite extracts obtained from a TRAMP murine model, involving androgen sensitive tumors and androgen insensitive tumors (CRPC). Comparisons of the fractional enrichments of ^{13}C labeled lactate, alanine, and glutamate between hormone sensitive versus insensitive TRAMP tumors provided information about which pathways were upregulated or downregulated by the onset of therapeutic resistance.

2. Materials and Methods

a. TRAMP Murine Model

The TRAMP murine model is known to pathologically and metabolically model the progression of human prostate cancer, particularly in regards to progression from an androgen sensitive to insensitive state[12]–[14]. All TRAMP studies were performed according to a protocol approved by the UCSF Institutional Animal Care and Use Committee. The animals were imaged initially on a preclinical MRI scanner to obtain a baseline tumor size, then underwent orchiectomy for castration, mirroring medicinal application of androgen deprivation therapy in patients. Serially after castration, ^1H anatomic imaging took place again to determine response to castration. CRPC was defined as a 20% increase in tumor volume in the post-castration images. In this study, a CRPC mouse was compared against an androgen sensitive high grade mouse to determine the changes that are associated with development of CRPC.

b. Uniformly-Labeled ^{13}C Glucose Infusion

Uniformly-Labeled ^{13}C ($\text{U-}^{13}\text{C}$) glucose was prepared according to the protocol developed by Lane et al [15]. $\text{U-}^{13}\text{C}$ glucose (Cambridge Isotope Laboratories) was mixed in sterile PBS to a 25% w/v ratio. After vigorous vortexing, the solution was passed through a 0.2 μm sterile filter.

Prior to infusion, the TRAMP mouse was anesthetized via nose cone delivery of isoflurane. 80 μL of room-temperature tracer solution was injected via tail vein. This was repeated a total of three times, with a 15 minute break in between injections, for a total injected volume of 240 μL . In between injections, the mouse was removed from anesthesia to limit impact on metabolism. 15

minutes after the last injection, the mouse was euthanized and tissue of interest was immediately removed and flash frozen in liquid nitrogen.

c. Metabolite Extraction

Metabolite extraction by methanol/chloroform/water was performed according to the procedure developed by Wu et al [16]. Frozen tissue samples were added to a round-bottom tube with 400 μ L of methanol and a stainless-steel bead. This was run in a TissueLyzer (Qiagen) in a cold room until the tissue was visually disrupted. The solution was transferred to a glass vial, where 400 μ L of chloroform and 360 μ L of water was added to a final ratio of 2:2:1.8. The vial was vortexed well and left in a cold room overnight to partition. The resulting layers were carefully separated, and the aqueous layer was lyophilized in preparation for NMR analysis.

Metabolite extraction via perchloric acid was adapted from Lin et al [8]. Tissue disruption was performed as above with 1 mL of 8% perchloric acid (Ricca Chemicals) instead of methanol. The homogenized solution was vortexed well, and then centrifuged for 10 minutes at 4°C. The supernatant was removed and neutralized via manual titration of potassium carbonate (Sigma-Aldrich), then allowed to sit on ice for 30 minutes. The extraction protocol was repeated on the pellet in order to maximize extraction efficiency. Once neutralized, the extracts were desalted through repeated lyophilization, resuspension, and centrifugation to remove as much neutralization salt as possible. Prior to NMR analysis, the two extractions were recombined in a single resuspension.

d. NMR Experiments

The dry tissue extracts were resuspended in 400 μ L D₂O. A NMR insert tube was filled with 0.11 mM TSP in D₂O. During NMR experiments, the insert tube was placed inside the NMR tube as a standard.

High resolution NMR was performed on an 800.13 MHz Bruker NMR scanner. After adjusting the tune, match, and shim, the spectrometer was locked onto the deuterium signal. NMR spectra obtained were a high-res 1D proton spectra, 1D proton spectra with the decoupling pulse turned off and turned on, TOCSY, and HSQC.

High-resolution 1D proton NMR was performed with 64 scans, 1 sec acquisition time, and 16776 points in the fid. 1D proton spectra with the decoupling pulse turned on or off were performed with 64 scans, 0.3 sec acquisition time, and 16776 points. TOCSY was performed with 4 scans, 512x4096 points, and a spectral width of 12 ppm in either direction. HSQC was performed with 8 scans, 4096x2048 points, and a spectral width of 120x6 ppm.

e. NMR Analysis

1D NMR analysis was performed using MNova (MestReNova 11.0.4, Mestrelab Research). Phase correction and baseline correction were performed automatically and manually adjusted if necessary, then spectra were zero-filled to 65536 points. For analysis, the TSP peak was normalized to its known concentration (0.24 mM in the untreated high grade extract, 0.11 mM in the CRPC extract) to allow for determination of concentrations. Peaks were identified by reference with the metabolite database at hmdb.com. 2D NMR analysis were performed on TopSpin (TopSpin 3.5 pl 7, Bruker). The spectra were manually phased. TOCSY data was zero-filled to a size of 2048x16384 points, giving a spectral resolution of 4.688284 Hz in the F1 dimension and

0.586877 Hz in the F2 dimension. HSQC data is zero-filled to a size of 16384x8192 points, giving a spectral resolution of 1.473669 Hz in the F1 dimension and 0.586877 in the F2 dimension. Peaks were identified by reference with the metabolite database at hmdb.com. Fractional enrichment was calculated as described earlier, with the equation:

$$F = \frac{A(\textit{satellites})}{A(\textit{satellites}) + A(\textit{central peak})}$$

3. Results

Both methanol/chloroform/water and perchloric acid extraction methods yielded spectra evident that metabolite extraction was successful. Comparison of the spectra indicated peak shifting in the perchloric acid spectrum, as seen in Fig 2. This was due to a different pH in perchloric extract spectrum, which can be fixed though better titration of the residual acid.. The perchloric acid extraction was more time consuming, as the salts produced during neutralization required several steps of desalting by lyophilization. This also introduced more chances of losing some sample during the desalting process. Thus, the perchloric acid extraction was less reproducible. In addition,

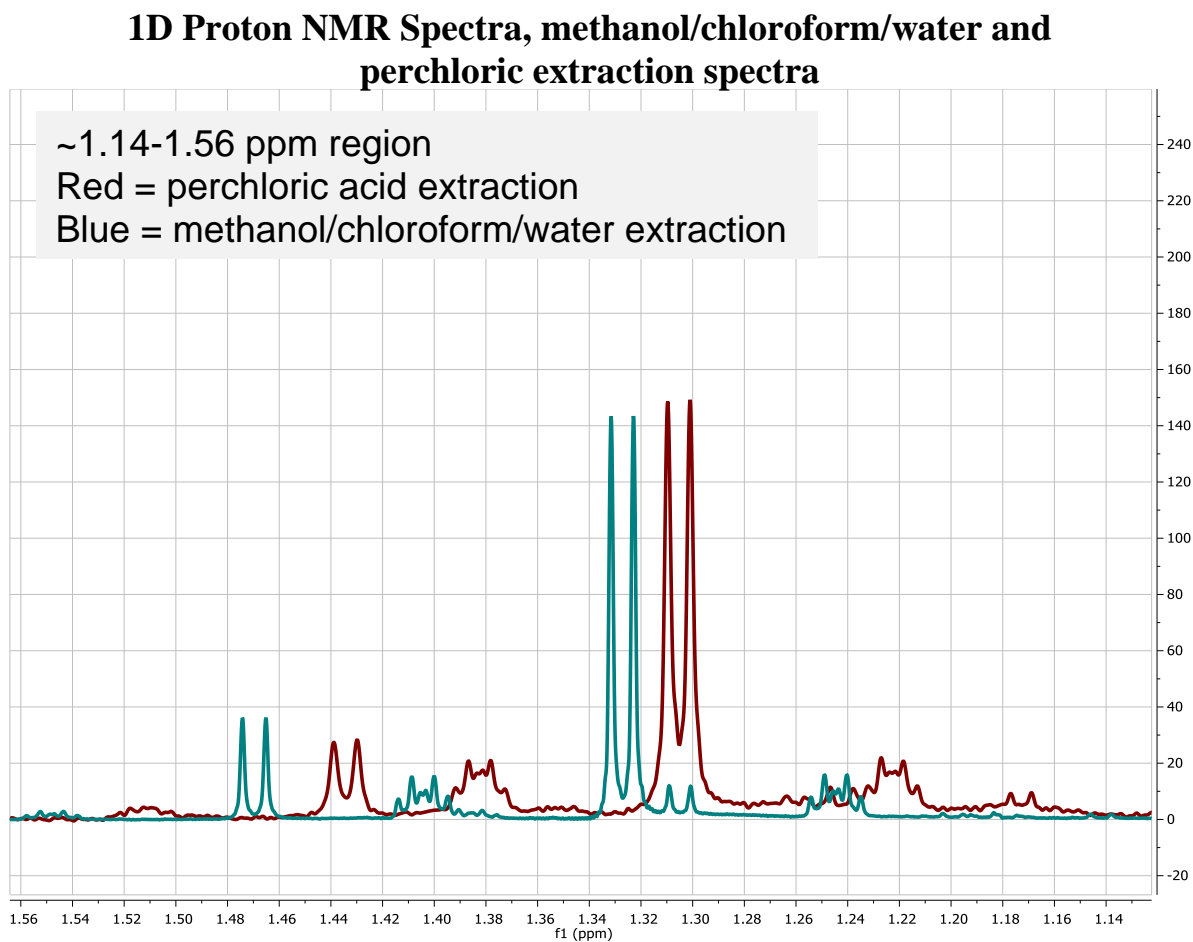


Figure 3: Alkyl region of the stacked 1D proton NMR spectra. The blue spectra is the methanol/chloroform/water extraction spectra, and the red spectra is that of the perchloric acid extraction.

the rationale for investigating perchloric acid, namely a cleaner baseline and higher metabolite extraction efficiency, were not realized in the spectra obtained in this study. For these reasons, the perchloric acid extraction method was not optimized further and all further data in this study utilized the methanol/chloroform/water extraction method.

^{13}C decoupling was used to collapse the ^{13}C satellite peaks into the ^{12}C unlabeled center peak, providing a method to obtain total concentration of the metabolite, as seen in Fig 4. Calculating the difference between the integrated peak areas of the lactate peaks between the spectra with the decoupling turned on and off, as seen in Table 1, revealed that ^{13}C decoupling was very efficient,

1D Proton NMR Spectra, Decoupling pulse on and off

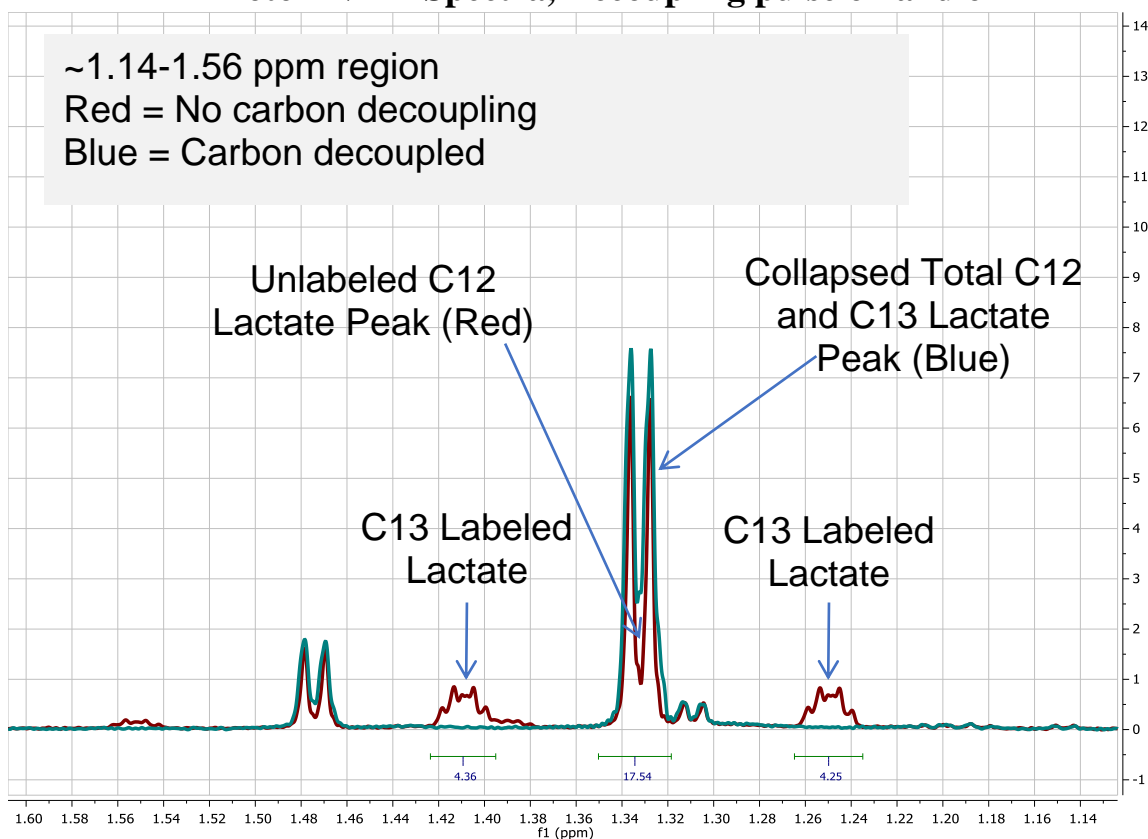


Figure 4: Alkyl region of stacked 1D proton NMR spectra. The red spectra has the decoupling pulse turned off, while the blue spectra has the decoupling pulse turned on.

Measured Metabolite Concentrations	
No Decoupling	Decoupled
Unlabeled: 3.21 mM	Collapsed: 4.44 mM
Labeled: 0.80 mM, 0.78 mM	Total: 4.44 mM
Total: 4.78 mM	
% Recovery: $4.44/4.78 * 100\% = 92.88\%$	

Table 1: Measured concentrations calculated from peak areas in the spectra with and without ^{13}C decoupling.

collapsing 92.88% of the total magnetization into the center peak. This indicates that the carbon decoupling pulse sequence is a viable method to analyze metabolite concentrations with relatively high sensitivity. However, regions of overlapping peaks require 2D NMR to analyze.

Analysis of TOCSY data, as seen in Fig 5, provided fractional enrichment for the three metabolites assayed in this study: ^{13}C labeled lactate, alanine, and glutamate. Region A, representing the lactate

TOCSY Spectra of Untreated High Grade and CRPC Extracts

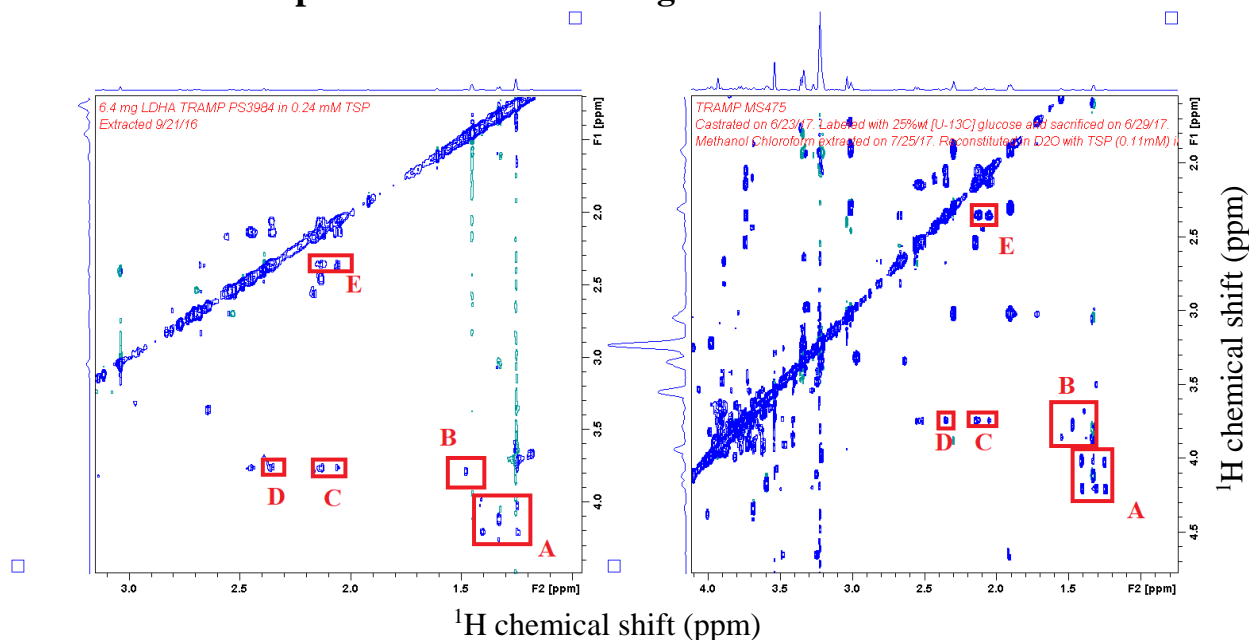


Figure 5: Untreated High Grade TOCSY data, left, and CRPC TOCSY Data, right, centered on region of interest. A is the lactate C2-C3 crosspeak, B is the alanine C2-C3 crosspeak, C is the glutamate C2-C3 crosspeak, D is the glutamate C2-C4 crosspeak, and E is the glutamate C3-C4 crosspeak.

Fractional Enrichment			
	Untreated High Grade	Castrate Resistant	% Change
Lactate	34.59%	41.30%	20.4%
Glutamate	8.16%	9.27%	13.6%
Alanine	**	37.13%	N/A

Table 2: Fractional enrichments for lactate, glutamate, and alanine. Alanine was undetectable in the high grade.

cross peak, displayed a X-shaped pattern. Figure 2 reveals that this pattern arises from a mixture of the C2 and C3 positions having ^{13}C labels and neither position being labeled. This makes sense as the uniformly labeled glucose will result in uniformly labeled lactate creating the satellites, and lactate produced from unlabeled glucose will produce the center peak; the C1 position, which should be labeled when produced from the labeled glucose, is not seen because it has no attached protons. As seen in Table 2, fractional enrichment increased for all three of the metabolites, to differing degrees. Alanine demonstrated the most marked change. In hormone sensitive high grade extract, no alanine satellites were detectable in the TOCSY data, suggesting that there was no labeling of alanine or the amount of labeling was too low to be detected in the TOCSY experiment. In contrast, the CRPC extract TOCSY had easily visible alanine satellites, corresponding to a fractional enrichment of 37.13%. Lactate and glutamate also displayed increased fractional enrichments to a lesser degree. Lactate had a 20.4% change, and glutamate had a 13.6% change. This points to an increase in flux in all three pathways during the shift from high grade prostate cancer to CRPC.

This is supported by the HSQC data, seen in Fig 6. The data in Fig 7 indicates that the relative increase in flux in glycolysis and amino acid synthesis was much greater than the increase in flux in the TCA cycle, despite all three pathways exhibiting an increased fractional enrichment.

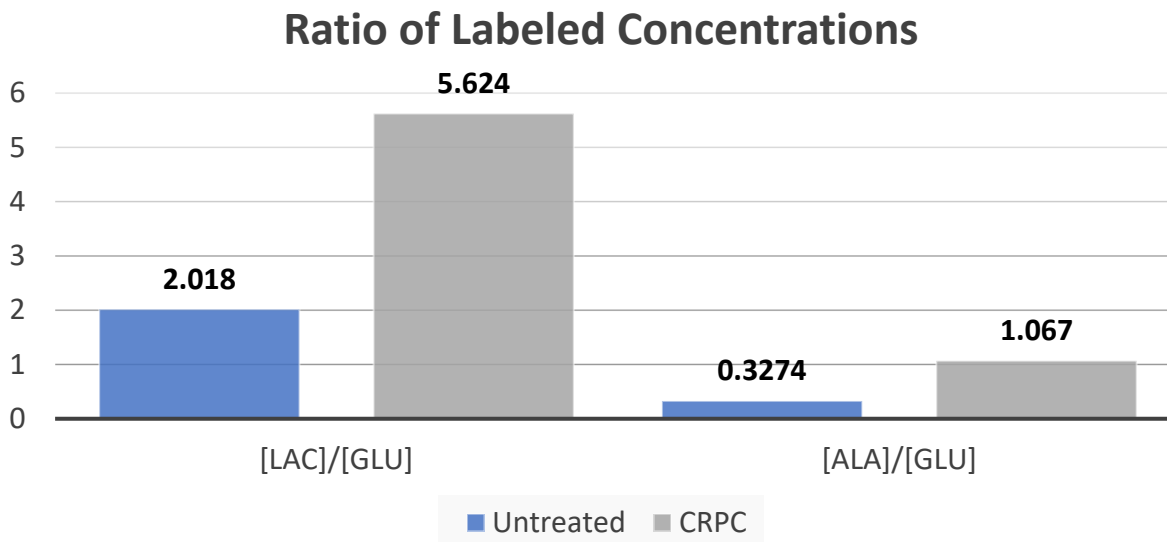


Figure 6: Comparisons of relative concentration ratios between untreated high grade and CRPC extracts

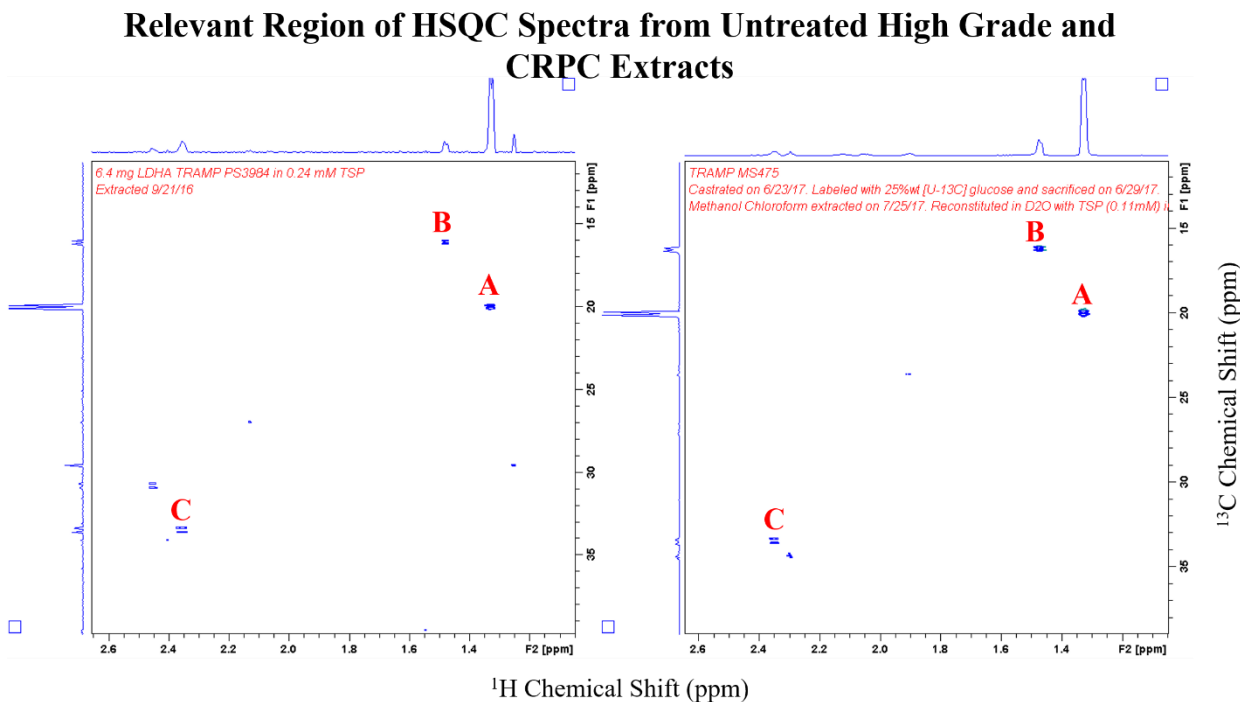


Figure 7: Relevant regions of HSQC spectra, with the spectra from the untreated high grade on the left and the CRPC on the right. A is the lactate C3 cross peak, B is the alanine C3 cross peak, and C is the glutamate C4 cross peak.

4. Discussion

One key future direction is to increase the sample size; this study was performed with only a sample size of one in each of the androgen sensitive high grade and CRPC groups. Increasing the number of animals studied is necessary in order to demonstrate that these changes in metabolic flux are reproducible and significant. . Both the magnitude of and reproducibility of these flux changes are important for selecting the best combination of hyperpolarized ^{13}C labeled metabolic probes used in future patient studies. Additionally, the metabolic data, in addition with expression data, can be mathematically modeled to supplement the relatively simplistic fractional enrichment analysis.

Should these results hold significance under further scrutiny, investment into optimizing hyperpolarized probes will be the next step in translating these results into tangible benefits to patient care. Hyperpolarized $[1-^{13}\text{C}]$ pyruvate is already being used in the clinic, and has the ability to look at the flux through LDH to produce $[1-^{13}\text{C}]$ ctate and through alanine transaminase to form $[1-^{13}\text{C}]$ anine. However, the label in the C1 position is lost as ^{13}C bicarbonate prior to entry to the TCA cycle, and so probing the TCA cycle and glutamate will require the addition of hyperpolarized $[2-^{13}\text{C}]$ pyruvate to the HP ^{13}C MRI exam, in order to probe the flux trough the TCA cycle through the production of $[5-^{13}\text{C}]$ glutamate. A co-polarization of both probes may prove to be a good method of pinpointing the development of therapeutic resistance and onset of CRPC in patients.

5. Conclusion

This study proposed that introduction of a stable ^{13}C labeled metabolic substrate, uniformly labeled glucose, would provide valuable information on the relative activities of three key metabolic pathways. The process of ^{13}C labeled substrate infusion and metabolite extraction by methanol/chloroform/water produces an extract of high enough quality for high resolution 1D and 2D NMR techniques. The carbon decoupled/undecoupled 1D and 2D NMR techniques provided complimentary methods to look at the metabolic fate of the ^{13}C label. Using these techniques, this study found that increases in the aerobic glycolysis, amino acid synthesis, and TCA cycle pathways are associated with a progression of prostate cancer from an androgen sensitive cancer to a lethal androgen insensitive phenotype (CRPC) after initiation of ADT. The findings of this preliminary study are being confirmed by reproducing the 1D and 2D NMR metabolomics measurements. If these *ex vivo* metabolic flux results prove reproducible, subsequent serial *in vivo* HP ^{13}C MRI studies using co-polarization of $[1-^{13}\text{C}]$ pyruvate and $[2-^{13}\text{C}]$ pyruvate will be performed in TRAMP mice at baseline and after ADT. The result of these studies will establish the utility of this combination of probes for future patient studies.

6. References

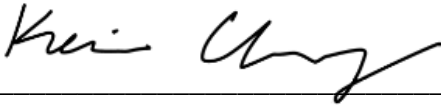
- [1] R. L. Siegel, K. D. Miller, and A. Jemal, “Cancer statistics, 2017,” *CA. Cancer J. Clin.*, vol. 67, no. 1, pp. 7–30, 2017.
- [2] Y. Ceder, A. Bjartell, Z. Culig, M. A. Rubin, S. Tomlins, and T. Visakorpi, “The Molecular Evolution of Castration-resistant Prostate Cancer.,” *Eur. Urol. Focus*, vol. 2, no. 5, pp. 506–513, Dec. 2016.
- [3] M. Katsogiannou, H. Ziouziou, S. Karaki, C. Andrieu, M. Henry de Villeneuve, and P. Rocchi, “The hallmarks of castration-resistant prostate cancers,” *Cancer Treat. Rev.*, vol. 41, no. 7, pp. 588–597, Jul. 2015.
- [4] F. Saad and S. J. Hotte, “Guidelines for the management of castrate-resistant prostate cancer.,” *Can. Urol. Assoc. J.*, vol. 4, no. 6, pp. 380–4, Dec. 2010.
- [5] O. Warburg, “On the Origin of Cancer Cells,” *Science (80-.)*, vol. 123, no. 3191, 1956.
- [6] J. H. Ardenkjaer-Larsen *et al.*, “Increase in signal-to-noise ratio of >10,000 times in liquid-state NMR.”
- [7] J. Kurhanewicz *et al.*, “Analysis of cancer metabolism by imaging hyperpolarized nuclei: prospects for translation to clinical research.,” *Neoplasia*, vol. 13, no. 2, pp. 81–97, Feb. 2011.
- [8] C. Y. Lin, H. Wu, R. S. Tjeerdema, and M. R. Viant, “Evaluation of metabolite extraction strategies from tissue samples using NMR metabolomics.”
- [9] T. W.-M. Fan, “Considerations of Sample Preparation for Metabolomics Investigation,” 2012, pp. 7–27.

- [10] A. N. Lane, T. W. -M. Fan, and R. M. Higashi, "Isotopomer-Based Metabolomic Analysis by NMR and Mass Spectrometry," 2008, pp. 541–588.
- [11] A. N. Lane and T. W.-M. Fan, "Quantification and identification of isotopomer distributions of metabolites in crude cell extracts using ^1H TOCSY," *Metabolomics*, vol. 3, no. 2, pp. 79–86, May 2007.
- [12] J. Gingrich, R. Barrios, B. Foster, and N. Greenberg, "Pathologic progression of autochthonous prostate cancer in the TRAMP model."
- [13] P. J. Kaplan-Lefko *et al.*, "Pathobiology of autochthonous prostate cancer in a pre-clinical transgenic mouse model," *Prostate*, 2003.
- [14] N. M. Greenberg *et al.*, "Prostate cancer in a transgenic mouse," *Med. Sci.*, vol. 92, pp. 3439–3443, 1995.
- [15] A. N. Lane, J. Yan, and T. W.-M. Fan, " ^{13}C Tracer Studies of Metabolism in Mouse Tumor Xenografts," *Bio-protocol*, vol. 5, no. 22, p. bio-protocol.org/e1650, Nov. 2015.
- [16] H. Wu, A. D. Southam, A. Hines, and M. R. Viant, "High-throughput tissue extraction protocol for NMR- and MS-based metabolomics," *Anal. Biochem.*, vol. 372, no. 2, pp. 204–212, Jan. 2008.

Publishing Agreement

It is the policy of the University to encourage the distribution of all theses, dissertations, and manuscripts. Copies of all UCSF theses, dissertations, and manuscripts will be routed to the library via the Graduate Division. The library will make all theses, dissertations, and manuscripts accessible to the public and will preserve these to the best of their abilities, in perpetuity.

I hereby grant permission to the Graduate Division of the University of California, San Francisco to release copies of my thesis, dissertation, or manuscript to the Campus Library to provide access and preservation, in whole or in part, in perpetuity.

Author Signature  Date Oct 1, 2017